

Sunspot models with bright rings

L. L. Kitchatinov^{1,2*} and G. Rüdiger²

¹Institute for Solar-Terrestrial Physics, Irkutsk, Russia

²Astrophysikalisches Institut Potsdam, Germany

*Email: lkitchatinov@aip.de

Abstract. A theoretical sunspot model is provided including magnetic suppression of the diffusivities and also a strong stratification of density and temperature. Heat diffusion alone with given magnetic field and zero mean flow only produces (after a very long relaxation time) dark spots without any bright ring. Models with full dynamics of both field and flow, however, provide rings and also the observed correlation of ring temperature excess and the spot size. The rings are formed as the result of heat transport by the resulting flow system *and* increased thermal diffusivity due to reduced magnetic quenching around spots.

1 Introduction

Measurements have shown the existence of bright rings around sunspots (Bonnet et al. 1978; Rast et al. 1999, 2001). The rings appear one spot radius beyond the spots and are reported to be about 10 K warmer than the photosphere. There is a clear trend that larger spots have brighter rings. We shall discuss in the following whether simple mean-field models of more or less flat sunspots do develop such rings or not.

2 A simple model

The model concerns a horizontal layer with top and bottom at depths d_{top} and d_{bot} below the photosphere. In our computations $d_{\text{top}} = 1$ Mm is fixed, slightly beneath the typical depth of Wilson depression. The fluid is assumed to be a perfect gas. Density and temperature at the top ($\rho_{\text{top}}, T_{\text{top}}$) and bottom ($\rho_{\text{bot}}, T_{\text{bot}}$) boundaries are prescribed with the solar structure model by Stix & Skaley (1990). The reference atmosphere is approximated by adiabatic profiles,

$$T = T_{\text{top}} + \frac{g}{C_p} (D - z), \quad \rho = \rho_{\text{top}} \left(\frac{T}{T_{\text{top}}} \right)^{\frac{1}{\gamma-1}}. \quad (1)$$

Here the gravity is $g = 2.74 \cdot 10^4$ cm s⁻², $D = d_{\text{bot}} - d_{\text{top}}$ is the layer depth (here 15 Mm), z is the vertical coordinate, C_p and γ are specific heat and adiabaticity index defined by the condition that the bottom temperature and density are exactly reproduced, i.e.

$$C_p = \frac{gD}{T_{\text{bot}} - T_{\text{top}}}, \quad \gamma = 1 + \frac{\ln(T_{\text{bot}}/T_{\text{top}})}{\ln(\rho_{\text{bot}}/\rho_{\text{top}})}. \quad (2)$$

The entropy equation with $S = C_v \log(P/\rho^\gamma)$ is

$$\rho T \left(\frac{\partial S}{\partial t} + \mathbf{u} \cdot \nabla S \right) = \nabla \cdot (\rho T \chi \nabla S). \quad (3)$$

The sunspot darkness is usually explained in terms of convective heat transport suppressed by magnetic field. Accordingly, the eddy diffusivities in the model depend on the magnetic field (cf. Rüdiger & Kitchatinov 2000). This dependence describes a steady decrease of the turbulent diffusivities with the magnetic field amplitude. Hence $\chi = \chi_T \varphi(\beta)$, where χ_T is nonmagnetic diffusivity and the quenching function

$$\varphi(\beta) = \frac{3}{8\beta^2} \left(\frac{\beta^2 - 1}{\beta^2 + 1} + \frac{\beta^2 + 1}{\beta} \arctan \beta \right) \quad (4)$$

depends on the field strength normalized to the energy equipartition value, $\beta = B/(\sqrt{\mu_0 \rho} u')$, u' is the rms turbulent velocity. Any anisotropy of the eddy diffusivities is neglected.

The depth profiles of the equipartition field, $B_{\text{eq}} = \sqrt{\mu_0 \rho} u'$, and the (nonmagnetic) diffusivities are written in accordance with the mixing-length approximation, which yields

$$\chi_T(z) = \chi_0 \left(\frac{T}{T_{\text{top}}} \right)^{\frac{3\gamma-4}{3(\gamma-1)}}, \quad B_{\text{eq}}^2 = B_0^2 \left(\frac{T}{T_{\text{top}}} \right)^{\frac{1}{3(\gamma-1)}}, \quad (5)$$

where T has been defined in (1) while χ_0 and B_0 are the thermal diffusivity and the equipartition field on the top boundary. A marginal value for thermal convection, $\chi_0 = 1.4 \cdot 10^{13} \text{ cm}^2/\text{s}$, was taken for the diffusivity, and $B_0 = 500 \text{ Gauss}$. The density runs from $2.02 \times 10^{-6} \text{ g/cm}^3$ at the top to $1.8 \times 10^{-3} \text{ g/cm}^3$ at the bottom, and the temperature varies from 14,000 K to 120,000 K.

The horizontal boundaries are stress-free and impenetrable. For the magnetic field a vacuum condition is used for the top while the field is assumed vertical on the bottom. Thermal conditions are the black-body radiation on the top and constant heat flux ($F_0 = 6.27 \cdot 10^{10} \text{ g s}^{-3}$) at the bottom. If wall boundaries are used we assume zero stress, zero normal velocity, and superconductor outside.

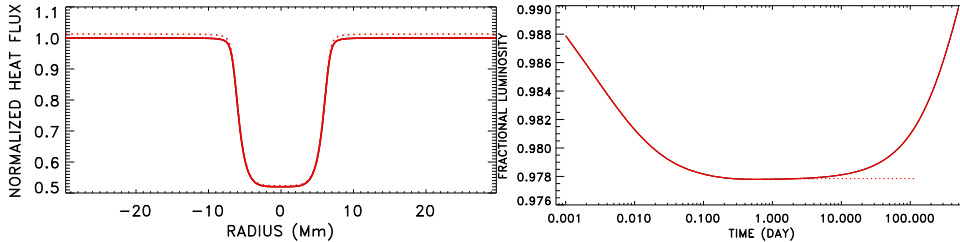


Figure 1. Left: Profiles of surface brightness normalized to F_0 after 1 day (solid) and after about 500 days (dotted) for vanishing heat flux across the wall boundary. Right: Time dependence of the normalized total irradiance at the top. The thermal conditions on the side wall are $F_r = 0$ (solid) and $\partial T/\partial t = 0$ (dotted).

A simplified model was used to probe the possibility of reproducing bright rings by heat transport alone. In this model the velocity is put to zero, the spot-like structure of the magnetic field is prescribed and stationary and the diffusion equation for the entropy is solved. It

is a rather flat spot with an aspect ratio $a = 2$. The spot of this model has a magnetic flux of $3 \cdot 10^{21}$ Mx and a depth of about 10 Mm.

The surface brightness at the initial state is uniform and equals F_0 . The brightness of the region occupied by magnetic field decreases due to magnetic quenching of the thermal diffusivity. The normalized surface brightness approaches the profile shown by the solid line in Fig. 1 (left panel) already after several hours and varies slowly after this time. The profile does not show any bright ring.

The further evolution depends on the thermal conditions imposed on the wall boundary. The boundary condition (zero heat flux across the boundary) ensures that in the steady state the total irradiance from the surface equals the heat supply at the bottom ($\pi R^2 F_0$). In the steady solution the heat flux blocked by the spot can reemerge *for flat spots* as a bright ring (Eschrich & Krause 1977). Figure 1 (right) shows that the luminosity does indeed recover after the initial reduction but it needs a very long time which is of the order of the Kelvin-Helmholtz time ($\tau_{KH} \sim 10$ yrs for our model).

The reason for this long time scale is the high heat capacity of the solar interior. The time passed before the rise in the surface irradiance can be seen is much longer than lifetimes of sunspots. Steady solutions of the heat transport equation are thus not relevant for sunspots. Also flatter spot models do not show any bright rings.

3 A new MHD sunspot model

For a more consistent MHD model for sunspots we work with the anelasticity condition, $\nabla \cdot (\rho \mathbf{u}) = 0$, and the complete momentum equation together with the induction equation

$$\frac{\partial \mathbf{B}}{\partial t} = \nabla \times (\mathbf{u} \times \mathbf{B} - \eta \nabla \times \mathbf{B}). \quad (6)$$

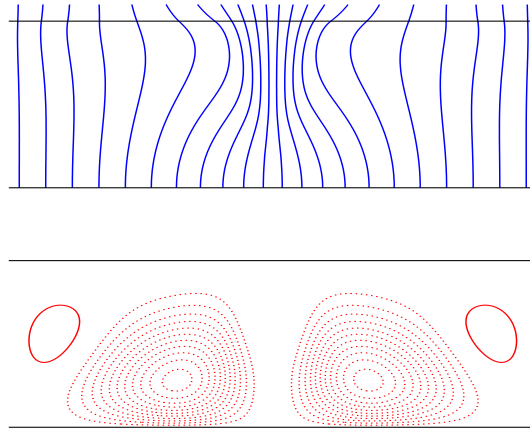


Figure 2. Field lines (top) and streamlines (bottom) after 3 days for an initial field of 600 Gauss. The dotted streamlines mean the flow convergent on the top and divergent on the bottom. The depth of the simulated spot is comparable to its diameter. The surface flow is convergent near the spot but divergent at larger distances.

Amplitudes of the initial uniform field of several hundred Gauss are considered. Magnetic diffusivity and eddy viscosity are assumed to follow the same magnetic quenching expressions as in Eq. (4).

The vertical size of the simulated spots is comparable to their diameter. The resulting mean ‘meridional circulation’ is convergent on the top near the spots and it makes down-drafts beneath the spots in agreement with results of heliotomography (Fig. 2, bottom). The amplitude of the flow is about 800 m s^{-1} . The flow direction becomes divergent at larger radial distances. The field strength in the spot is about 2700 Gauss. Brightness and field strength are almost uniform in the central parts of the spots but they change rapidly with radius beyond the ‘umbra’.

The radial heat-flux profiles show bright rings around the spots. Our rings are somewhat brighter than the observed rings.

A comparison of Figs. 2 and Fig. 3 shows that the position of the ring maximum is at the radius where the horizontal surface flow changes its direction and an upwards directed sub-surface flow appears. At the same radius the surface field strength has a minimum. Hence, the upward flow carries extra heat from beneath *and* the reduced field strength increases the diffusive heat flux due to reduced magnetic quenching of the thermal diffusivity (4). If the flow is switched off to probe its contribution to the bright rings they do not disappear. We conclude that both the flow and the reduced diffusivity quenching contribute to the resulting bright rings. The contribution by the circulation should basically be steady. Observations can help to decide between the two possible explanations for the rings by finding out whether the rings around big spots are decaying on a time scale of some days or not.

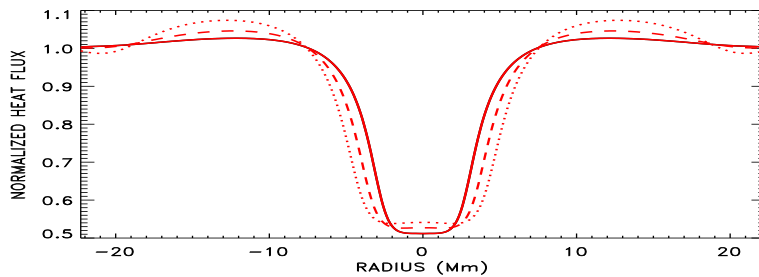


Figure 3. Surface brightness normalized to F_0 for the time of 3 days in the runs for initial fields of 400 (full line), 500 (dashed), and 600 Gauss (dotted). All runs show bright rings which are more pronounced for larger spots.

References

- Bonnet, R. M., Lemaire, P., Vial, J. C., et al. 1978, *ApJ*, 221, 1032
 Eschrich, K.-O. & Krause, F. 1977, *Astron. Nachr.*, 298, 1
 Kitchatinov, L. L., Pipin, V. V., & Rüdiger, G. 1994, *Astron. Nachr.*, 315, 157
 Rast, M. P., Fox, P. A., Lin, H., et al. 1999, *Nature*, 401, 678
 Rast, M. P., Meisner, R. W., Lites, B. W., et al. 2001, *ApJ*, 557, 864
 Rüdiger, G. & Kitchatinov, L. L. 2000, *Astron. Nachr.*, 321, 75
 Stix, M. & Skaley, D. 1990, *A&A*, 232, 234